NRL Report 6696

A Matrix-Fed Circular Array for Continuous Scanning

B. Sheleg

Electronics Division

Microwave Antennas and Components Branch
Electronics Division

April 2, 1968

NAVAL RESEARCH LABORATORY
Washington, D.C.

This document has been approved for public release and sale; its distribution is unlimited.

CONTENTS

Abstract	ii
Problem Status	ii
Authorization	ii
INTRODUCTION	1
THEORY OF OPERATION	1
PATTERN CALCULATION	6
SYNTHESIS OF APERTURE DISTRIBUTIONS	15
EXPERIMENTAL PROGRAM	19
CONCLUSIONS	26
ACKNOWLEDGMENTS	27
REFERENCES	27

ABSTRACT

If the radiators of a circular array are connected to the outputs of a Butler matrix, a focused radiation pattern can be formed by establishing the proper current distribution on the inputs of the Butler matrix. Further, if the amplitudes of the input currents are held fixed, the pattern can be scanned through 360 degrees in azimuth by the operation of phase shifters alone, just as the pattern of a linear array is scanned by varying the phases of the element currents. One explanation of this is based on the assumption that the pattern can be written as the sum of a finite number of uniform pattern modes and that the relative phases and amplitudes of these modes can be adjusted to form a narrow beam. Then the beam is scanned by adjusting the currents feeding the Butler matrix. This is only qualitatively correct; the patterns calculated from the actual current distribution established on the array by the matrix differ from the patterns formed from the ideal modes. There is reasonable agreement between the calculated patterns and those obtained experimentally with a 32-element array of dipoles used to demonstrate how a beam could be formed and then scanned. The inputs to the Butler matrix required to achieve a prescribed cophasal sector distribution on the array are determined from the synthesis procedure of Davies with the corresponding changes in the current distribution on the array for other beam positions.

PROBLEM STATUS

This is an interim report; work continues on other phases of the problem.

AUTHORIZATION

NRL Problem R08-38
Project A36533818/6521/F001-02-02

Manuscript submitted January 18, 1968.

A MATRIX-FED CIRCULAR ARRAY FOR CONTINUOUS SCANNING

INTRODUCTION

Antennas consisting of radiating elements arrayed on a circle have been studied and have been used for many years, but recent developments in switching and phase shifting have led to a renewed interest in them. The appeal of the circular array is that, because of its symmetry, it can be used to scan a beam in discrete steps through a full 360 degrees without the variations in gain and pattern shape that occur when four linear arrays are used, each scanning through a single quadrant. The purpose of this study was to determine some of the possibilities and also the limitations of scanning with circular arrays and, in particular, to demonstrate the use of the Butler matrix in feeding the elements of the array. The idea of using a Butler matrix for this purpose is due to Shelton (1) who showed that it permitted the formation of a narrow radiated beam which could then be scanned essentially as is the beam from a linear array — by the operation of phase shifters alone.

The operation of a Butler-matrix-fed circular array ("multimode array") is first described as the summation of the various far-field "modes" that are generated by the excitation of individual inputs to the matrix. This explanation, used by Shelton, assumes a continuous current distribution on the circle, although the antenna is actually an array; however approximate, it gives a good insight into the operation of a multimode array. A more satisfying analysis uses the distribution of currents impressed on the elements by the Butler matrix. In addition, calculations were made to show how the radiation pattern of the multimode array varies as it is scanned continuously, rather than in discrete steps.

The experimental portion of this program was performed at L-band with circular arrays of 16 and 32 elements, using dipoles around a conducting cylinder for radiators. All the arrays were fed from Butler matrices, and scanning was accomplished by mechanical line-stretchers. Several different corporate structures, providing various amplitude tapers over the illuminated sector of the array, were used to show that the sidelobe level could be controlled. There was reasonable agreement between the measured and the calculated patterns.

THEORY OF OPERATION

The principles involved in scanning a multimode array are most easily seen by considering not an array, but a continuous distribution of current. When this distribution is expressed as a Fourier series, in general infinite, each term represents a current mode uniform in amplitude but having a phase varying linearly with angle. The radiation pattern of each mode has the same form as the current mode itself, and these pattern mode are the Fourier components of the radiation pattern of the original distribution. The expression of the radiation pattern as the sum of modes of this form is then seen to be analogous to the summation of the contributions made to the pattern of a linear array by its elements, so the operation of a multimode array can be explained by referring to an equivalent linear array.

Consider, as in Fig. 1, a continuous cylindrical sheet of vertical currents of infinitesimal height, and let $I(\alpha)$, where α is the angular variable, be the complex current distribution around the circle. The far-field pattern $E(\theta, \phi)$ is given by

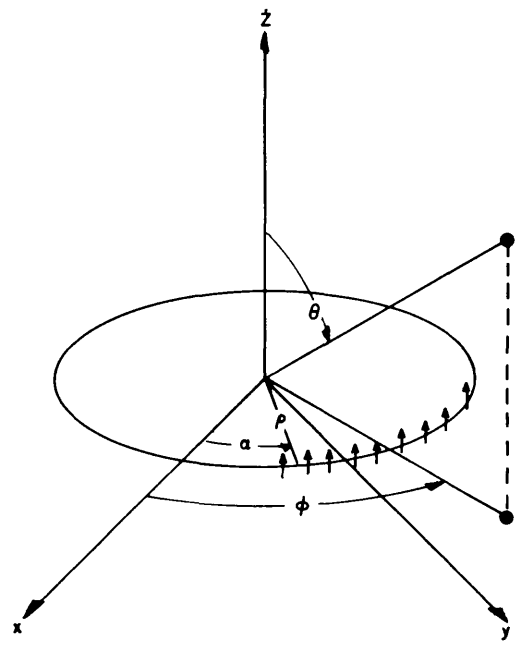

Fig. 1 - Coordinates for a continuous cylindrical sheet of vertical current elements

$$E(\theta, \phi) = K \int_0^{2\pi} I(\alpha) \sin\theta \exp\left[j \frac{2\pi\rho}{\lambda} \sin\theta \cos(\phi - \alpha)\right] d\alpha, \tag{1}$$

where K is a constant, $\sin\theta$ is the element factor, and the exponential represents the relative space phase of the current elements. If $I(\alpha)$ is expressed as a complex Fourier series

$$I(\alpha) = \sum_{n=-\infty}^{\infty} I_n \, e^{jn\alpha} \tag{2}$$

and is substituted into Eq. (1), it is found upon term-by-term integration (2) that

$$E(\theta, \phi) = 2\pi K \sin\theta \sum_{n=-\infty}^{\infty} I_n \, j^n \, J_n\left(\frac{2\pi\rho}{\lambda} \sin\theta\right) e^{jn\phi}. \tag{3}$$

If attention is restricted to the plane of the array $\theta = \pi/2$ the radiation pattern is

$$E(\phi) = \sum_{n=-\infty}^{\infty} C_n \, e^{jn\phi}, \tag{4}$$

where the C_n are complex constants given by

$$C_n = 2\pi K\, j^n\, I_n\, J_n\left(\frac{2\pi\rho}{\lambda}\right) . \tag{5}$$

It is seen from Eqs. (2) and (4) that if the current distribution is expressed as the sum of current modes of the form $e^{jn\alpha}$, the radiation pattern in the plane of the antenna is the sum of far-field pattern modes of precisely the same form, $e^{jn\phi}$, there being a one-to-one correspondence between current modes and pattern modes. Each current mode (with its corresponding field mode) has uniform amplitude with phase varying linearly in azimuth. The total excursion around the circle is $2\pi n$ radians. Although each pattern mode has exactly the same form as the current mode which is its source, it should be noted that the relative phases of the pattern modes are not necessarily the same as the relative phases of the current modes, i.e., if two current modes have the same phase at some angle, say at $\alpha = 0$, the corresponding pattern modes are not, in general, in phase at $\phi = 0$. In fact, for the ring of vertical current elements, it may be seen from Eq. (5) that the Nth and the $(N+1)$th pattern modes differ in phase by $\pi/2$ at that angle for which the corresponding current modes are in phase.

Another property peculiar to this configuration is that certain modes might make no contribution to the pattern in the plane of the circle. This happens when the circle is of the proper diameter to cause one of the Bessel functions of Eq. (3) to vanish. For example, if the circumference of the ring were 8.65λ, J_0 would vanish in the plane $\theta = \pi/2$, and there would be no zero mode in that plane. This creates no problem in computing the radiation pattern for a given current distribution, but it would severely limit pattern synthesis if this pattern mode were not available.

The possibility that certain pattern modes vanish exists because the vertical current element is omnidirectional in azimuth; therefore, all elements on the ring make contributions of equal magnitude at each azimuth angle, and, with the proper combination of diameter and phase progression, the elevation pattern will have a null in the plane $\theta = \pi/2$. If the radiating elements are directive in the azimuth plane, as is true for most practical antennas, only certain elements (usually those that are optically visible) are effective at any particular angle, and it is found that none of the modes of interest vanish in the plane of the array.

Suppose now that the current distribution $I(\alpha)$ is the sum of just a finite number of current modes $I_n e^{jn\alpha}$ with $-N \leqq n \leqq N$. The radiation pattern is given by

$$E(\phi) = \sum_{n=-N}^{N} C_n\, e^{jn\phi}, \tag{6}$$

and C_n, the relative phase and amplitude of each pattern mode, can be set by adjusting I_n, the relative phase and amplitude of the corresponding current mode. This is nearly identical to the formulation for linear arrays. A linear array of $2N+1$ isotropic elements with interelement spacing a has a radiation pattern given by

$$E(u) = \sum_{n=-N}^{N} A_n\, e^{jnu}, \tag{7}$$

where $u = ka \sin\phi$, ϕ is the angle off broadside, and A_n is the current on the nth element. Equations (6) and (7) show the similarity of the patterns of the circular current sheet and the linear array, with the role of the current mode in the circular array taken by the element in the linear array. One difference is that for the circular array the argument is ϕ, and for the linear array it is $ka \sin\phi$. A second difference is that equally excited elements in a linear array make contributions of equal magnitude to the radiation pattern,

but equally excited current modes do not contribute equally, because their elevation patterns are not identical. This results in differences in directivity in the plane of the antenna. For example, if in the antenna being considered (Fig. 1) it is desired that the pattern modes be equal in magnitude and be in phase at $\phi = 0$, the excitations of the current modes must be (from Eq. (5))

$$I_n = \frac{1}{2\pi K\, j^n\, J_n\left(\frac{2\pi\rho}{\lambda}\right)} . \tag{8}$$

Its radiation pattern is then given by

$$E(\phi) = \sum_{n=-N}^{N} e^{jn\phi}, \tag{9}$$

which may be summed to give the pattern characteristic of a uniform array

$$E(\phi) = \frac{\sin\left(\frac{2N+1}{2}\phi\right)}{\sin\frac{\phi}{2}} . \tag{10}$$

The beam can be scanned (in theory) by a linear variation of the phases of the mode excitations, just as the beam from a linear array is scanned by a linear variation of the element phases. If the phase difference between adjacent modes is ϕ_0 radians (multiplying I_n of Eq. (8) by $e^{-jn\phi_0}$), the resultant pattern is expressed as

$$E(\phi) = \frac{\sin\left[\frac{2N+1}{2}(\phi - \phi_0)\right]}{\sin\left(\frac{\phi - \phi_0}{2}\right)} , \tag{11}$$

which is the original pattern scanned ϕ_0 radians. Although the foregoing analysis was based on the particular example of a cylindrical sheet of infinitesimal current elements, the same reasoning applies to any circular antenna having similar pattern modes. The only difference in the analysis would be the particular relationship between the phases and amplitudes of the pattern modes and their respective current modes.

Various antennas have used the multimode principle in their operation. One was the multiterminal direction finder developed by the Stanford Research Institute (3) in which a zero mode (TEM mode with no azimuthal phase variation) and the ±1 modes (TE modes with $\pm 2\pi$ radians variation) were generated in a biconical horn to form a rotatable cardiod pattern. Another was the concentric loop array (4) of Schell and Bouche in which circular wire loops of circumference $\lambda, 2\lambda, \ldots, N\lambda$ were used for modes ±1, ±2, . . . , $\pm N$, respectively, with a small loop at the center for the zero mode. Both these antennas had the property that the radiated modes conformed precisely to the desired $e^{jn\phi}$ patterns. It is, in general, difficult to generate a number of such pure modes, but it was shown that concentric-ring arrays could be used to obtain good approximations (5). A concentric-ring antenna, shown in Fig. 2, consists of rings of radiating probes mounted between circular parallel plates. The center element radiates in the zero mode. Modes +1, +2, and +3 are established on rings 1, 2, and 3 by feeding each ring from an individual corporate structure which provides currents of uniform amplitude with phase varying linearly around the ring. The number of radiators in each ring is enough to make the radiation pattern conform, within some prescribed tolerance, to the desired $e^{jn\phi}$ pattern. Although the antenna described has only modes with a positive sense of phase variation, the modes may be combined in a corporate structure to give a directive pattern which may

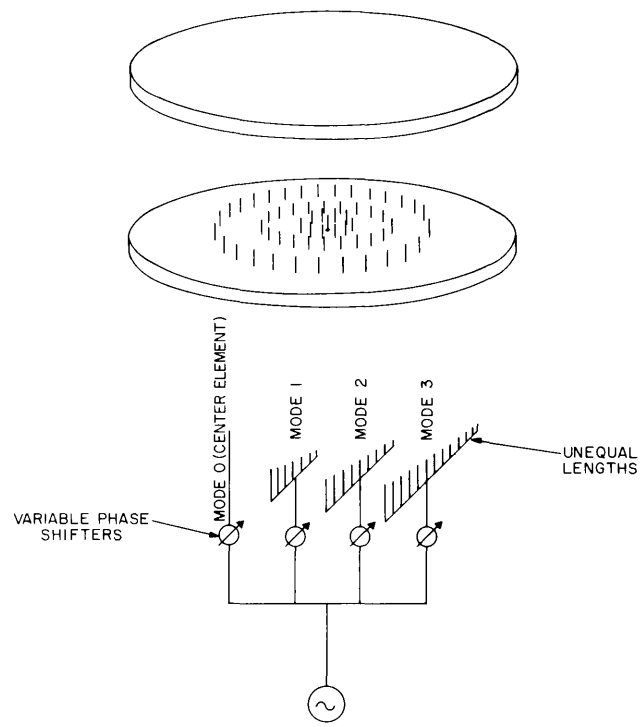

Fig. 2 - Concentric ring array

then be scanned by varying the phases of the inputs to the modes. The radiation pattern when the four modes have equal amplitude is

$$E(\phi) = e^{j(3\phi/2)} \frac{\sin 2\phi}{\sin(\phi/2)} \tag{12}$$

If both positive and negative modes are simultaneously established, there would be seven modes which could be added to give the pattern

$$E(\phi) = \frac{\sin(7\phi/2)}{\sin(\phi/2)}, \tag{13}$$

almost halving the beamwidth of the four-mode pattern.

As has been mentioned, Shelton noted that the complicated radiating structure of Fig. 2 was not necessary, but that it was possible on a single ring of N elements to excite simultaneously and independently all the modes, both positive and negative, from zero to $N/2$ by connecting the elements to the outputs of a Butler matrix. That this is true is evident from the definition of the Butler Matrix (6). This matrix is a lossless, passive network having N inputs and N outputs, where N usually is some power of 2. The inputs are isolated from one another, and a signal into any input results in currents of equal amplitude on all the outputs with phase varying linearly across the elements. Specifically, if N is even and the Kth input port is energized ($K = 0, \pm 1, \pm 2, \ldots, \pm(N-2)/2, N/2$), the difference in phase between adjacent output ports is $K(2\pi/N)$, and the total phase variation around a circular array connected to the Butler matrix would be $2\pi K$, which is the Kth mode. Hence, with the Butler matrix we may establish on the array the N current modes corresponding to $K = 0, \pm 1, \ldots, \pm(N-2)/2, N/2$, and, because the input ports are

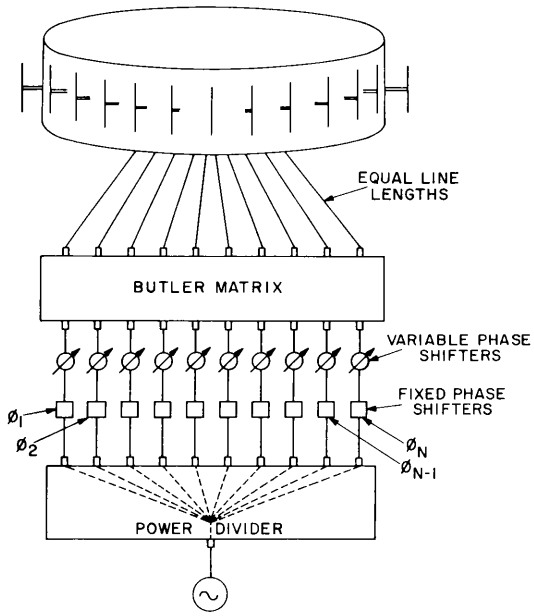

Fig. 3 - Schematic diagram of a scanning multimode array

isolated, the modes are independent. It should be noted here that there are Butler matrices that do not satisfy the definition given above and that cannot be used unmodified in a multimode array — these networks establish, across their outputs, linear phase progressions whose total variations are odd multiples of π radians. A matrix of this type can be changed to one having the proper modes by adding fixed phase shifts to all the output ports; if the N outputs are labeled $J = 1, 2, \ldots, N$, the phase shift applied to the Jth output is $J(\pi/N)$.

A schematic diagram of a scanning multimode array is shown in Fig. 3. The corporate structure is used to establish the desired amplitude distribution over the inputs to the Butler matrix. If all the modes were to be excited, the corporate structure would have N outputs. There is a variable phase shifter, used in scanning the beam, in each line connecting the corporate structure to the Butler matrix; in addition, there are fixed phase shifters to put all the pattern modes in phase at some desired azimuth angle. Obviously, the fixed phase shifters could be incorporated (and usually are) either in the corporate structure or in the variable phase shifters. The exact values of the fixed phase shifts can be determined experimentally or by calculating the mode patterns. Once the pencil-beam pattern is formed at some azimuth angle, it is scanned just as is a linear array, the mode amplitudes are held fixed, and a linear phase progression is set up on the mode inputs by operating the variable phase shifters.

PATTERN CALCULATION

Thus far, the explanation of a multimode array has been based on the summation of pattern modes of the form $e^{jK\phi}$. The summation could be exactly achieved with a continuous current sheet, or it could be approximated arbitrarily well with a ring array having a sufficient number of elements. For arrays fed from a Butler matrix, as many current modes can be established as there are elements, and it is not obvious how many of these modes have far-field patterns that fit the $e^{jK\phi}$ form sufficiently well. For example, in an N-element array the highest order mode $(K = N/2)$ has an element-to-element phase variation of π radians. By symmetry, its pattern must be scalloped, with N nulls and N peaks; therefore, it obviously cannot be used as a uniform mode.

To determine the quality of the modes established by the Butler matrix, a series of calculations was made, both of mode patterns and of pencil-beam patterns obtained by summing different numbers of modes. The arrays consisted of either 16 or 32 elements, and the interelement spacing was varied from 0.4 to 0.6λ. Two different element patterns were used; one was an approximation to the measured pattern of the elements that were actually used (dipoles around a cylinder) and the other was the exact pattern of an infinitesimal vertical current element in front of a conducting cylinder. The approximate pattern of the dipole in front of a cylinder is given by

$$A(\phi) = \frac{1}{2}(1 + \cos\phi), \tag{14}$$

where the phase was assumed constant in azimuth when referred to a point one-third the distance from the cylinder to the dipole. This assumption is reasonably good, at least in the unshadowed region. Mode patterns and pencil-beam patterns computed using Eq. (14) were in good agreement with those obtained using the exact pattern of the vertical current element, and no results for the latter have been included.

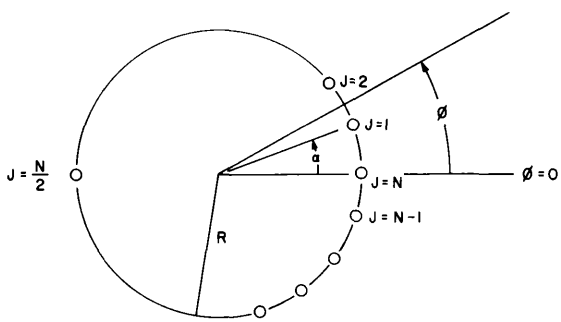

Fig. 4 - Geometry of the circular array

Consider, as in Fig. 4, a circular array of radius R with N elements equally spaced at $\alpha_J = J(2\pi/N)$, where $J = 1, 2, \ldots, N$. Referred to the center of the circle, the relative space phase of the Jth element is $(2\pi R/\lambda)\cos(\phi - \alpha_J)$, where only the plane of the array is considered. If the element pattern is $A(\phi - \alpha_J)$ and the current on the element is $A_J e^{j\psi_J}$, the radiation pattern of the array is given by

$$E(\phi) = \sum_{J=1}^{N} A_J e^{j\psi_J} A(\phi - \alpha_J) \exp\left[j\frac{2\pi R}{\lambda}\cos(\phi - \alpha_J)\right]. \tag{15}$$

Mode patterns were calculated from this equation with the element pattern given by Eq. (14) and, for the Kth mode, a current distribution given by $A_J = 1$, $\psi_J = 2\pi(KJ/N)$. Results are shown for a 32-element array, for which the modes correspond to $K = 0, \pm1, \pm2, \ldots, \pm15, 16$. The computed mode patterns for an array with 0.5-λ spacing are in Fig. 5 and show both the amplitude and a comparison of the computed phase with the ideal linear variation. It is seen that all modes up to ±10 are in substantial agreement with the ideal patterns, having at most a ±0.25-dB difference from a uniform pattern, with a maximum phase error of 3 degrees. Modes ±14, ±15, and 16 are poor approximations. Mode patterns were also computed for arrays with element spacings of 0.4 and 0.6λ. With the closer spacing, modes up to ±12 are close to ideal, and modes ±15 deviate about as much as did modes ±14 for the array with 0.5-λ spacing. For 0.6-λ spacing, modes up to ±9 are good, and mode 12 corresponds to mode 14 for 0.5-λ spacing. Table 1 lists the relative gains of all the pattern modes for 0.5-λ spacing and also their relative phases at $\phi = 0$ when the current modes are in phase at $\alpha = 0$ (i.e., at element 32). To form a narrow beam with its peak at $\phi = 0$, the pattern modes must be in phase in that direction; therefore, the phase differences between the modes must be accounted for, as shown in Fig. 3, by fixed phase shifts at the inputs to the Butler matrix. For modes nearly ideal, the phase differences of Table 1 would be used, but for a mode whose phase deviated significantly from the proper linear variation (such as mode 12 of Fig. 5) a best-fitting linear phase would be used to establish the proper correction.

The analysis of a circular array in terms of ideal modes is adequate for a qualitative description of its operation and does predict reasonably well the position and shape of the

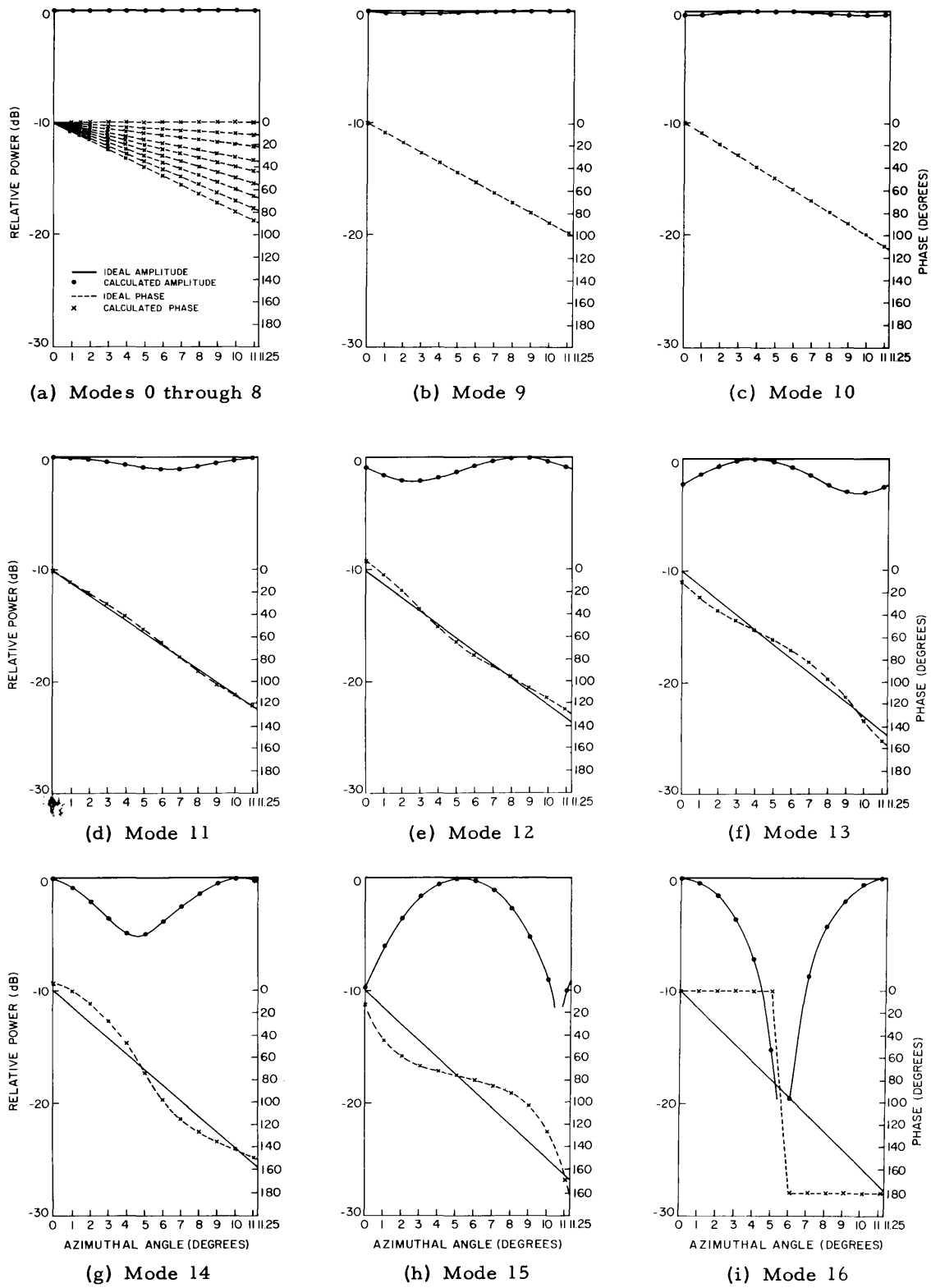

(a) Modes 0 through 8 (b) Mode 9 (c) Mode 10

(d) Mode 11 (e) Mode 12 (f) Mode 13

(g) Mode 14 (h) Mode 15 (i) Mode 16

Fig. 5 - Calculated mode patterns for a 32-dipole circular array compared with the ideal mode patterns

Table 1
The Relative Gains and Phases of the Pattern Modes of a 32-Element Array

Mode	Relative Gain (dB)	Relative Phase at $\phi = 0$ (degrees)
0	0.0	0.00
1	0.2	0.74
2	0.1	7.51
3	0.2	14.63
4	0.2	29.27
5	0.0	44.63
6	0.5	63.06
7	0.2	91.93
8	-0.5	115.35
9	0.8	144.56
10	1.0	-168.45
11	-0.5	-128.07
12	0.7	-105.74
13	3.5	-35.18
14	5.1	20.91
15	5.6	120.92
16	5.6	-172.05

main lobe but not the structure of the sidelobes. For a more accurate estimate, the current distribution on the array must be determined, and the pattern must then be calculated from Eq. (15). First assume that the N-element Butler matrix has all the current modes in phase at the Nth element if the mode inputs are fed in phase; this means that for the Kth mode the Jth element has phase $2\pi(KJ/N)$. Then, if $B_K e^{j\beta_K}$ is the current applied to the Kth input port, the resultant current $A_J e^{j\psi_J}$ on the Jth radiating element is given by

$$A_J e^{j\psi_J} = \frac{1}{\sqrt{N}} B_K e^{j\beta_K} e^{jKJ(2\pi/N)} . \tag{16}$$

If many input ports are simultaneously excited, the output currents may be added to give

$$A_J e^{j\psi_J} = \frac{1}{\sqrt{N}} \sum_K B_K e^{j\beta_K} e^{jKJ(2\pi/N)} . \tag{17}$$

This current distribution may then be substituted into Eq. (15) to give the radiation pattern expressed as

$$E(\phi) = \sum_{J=1}^{N} \left[\sum_K B_K e^{j\beta_K} e^{jJK(2\pi/N)} \right] A(\phi - \alpha_J) e^{j(2\pi R/\lambda)\cos(\phi - \alpha_J)} . \tag{18}$$

It is perhaps evident from the symmetry of the multimode array that the pattern shape does not change if the beam is scanned by some multiple of $2\pi/N$, the angle between elements. If, for example, the beam is to be scanned $M(2\pi/N)$ radians, where M is an integer, the mode amplitudes B_K are held constant but there must be a mode-to-mode phase difference of $M(2\pi/N)$; hence, the phase of the Kth mode becomes $\beta_K + KM(2\pi/N)$. When this is substituted into Eq. (17), the current on the Jth radiating element is found to be

$$A_J e^{j\psi_J} = \frac{1}{\sqrt{N}} \sum_K B_K e^{j\beta_K} e^{j(M+J)K(2\pi/N)}, \tag{19}$$

showing that the original current distribution has been moved, intact, M elements around the array.

To show the formation of the radiation patterns as the modes are superimposed, patterns of a 32-element array with 0.5-λ spacing were computed from Eq. (18) using the cardiod element pattern of Eq. (14). With uniform excitation of the Butler matrix inputs (all $B_K = 1$) and with phases corresponding to those in Table 1, the modes were successively excited and at each stage the radiation pattern was calculated, giving the series of patterns shown in Fig. 6. It can be seen that the beam narrows as more modes are added and that, until modes ±11 are reached, the far-out sidelobes decrease as they would if the modes were perfect. This improvement ceases as the higher modes are added; when all the modes but the 16th are included, the pattern is noticeably worse than when just the modes up to ±10 are used. The two patterns using modes up to ±10 and up to ±15 are compared in Fig. 7 with the patterns that would result if the corresponding numbers of ideal modes were summed. The agreement, when all the modes are used, is particularly poor in the region of the far-out lobes; when the less uniform modes (11 through 15) were not used the patterns for the discrete and continuous cases agreed everywhere to within 0.5 dB.

It is interesting to examine the current distribution that is established on the array when the Butler-matrix inputs are fed so as to produce a focused radiation pattern (as in Fig. 7). Since the radiating elements have directive patterns, it is reasonable to expect that the strongly excited elements would be on the side of the array in which the beam is directed and that their phases would be, to a degree, corrected to a line normal to the beam. A current distribution of this type is called "cophasal." From Fig. 8 the phase of the Jth element should then be

$$\frac{2\pi R}{\lambda}\left[1 - \cos\left(\phi_0 - J\,\frac{2\pi}{N}\right)\right], \tag{20}$$

where R is the radius of the array, ϕ_0 is the angle of the pattern peak, and $J(2\pi/N)$ is the angular position of the Jth element. The current distribution on the array when all the modes but the 16th are fed with uniform amplitudes is shown in Table 2. It is seen that about 95% of the total power is radiated by the 13 elements nearest element 32 (which is in the direction of the pattern peak) and that the currents on 11 of these differ from the phase required for a cophasal distribution by less than 20 degrees, while the end elements differ by 34 degrees.

The sidelobes from a linear array can be lowered by tapering the amplitude distribution over the array, and, by analogy, the same should be true for a circular array if the mode amplitude distribution is tapered. With the phases again as in Table 1, a cosine taper was applied to the mode inputs (i.e., $B_K = \cos(K\pi/32)$), and the patterns were computed as modes were added successively (Fig. 9). Figure 10 is a comparison of the final pattern, when all the modes were used, with the pattern that would result if the modes were ideal. This shows that the sidelobe level has indeed been reduced but not to the level that would be obtained with perfect modes. The corresponding current distribution

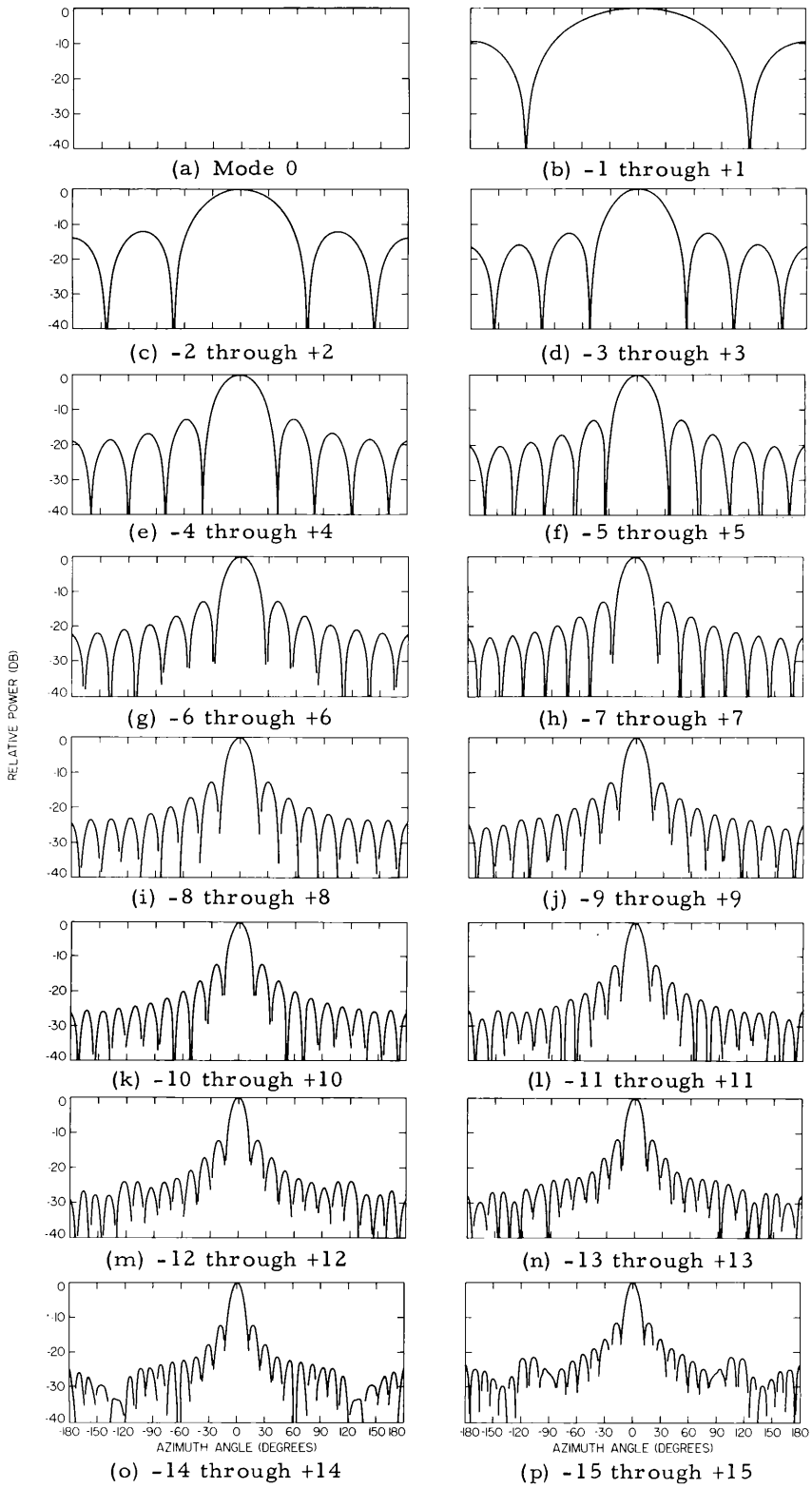

Fig. 6 - Mode-by-mode buildup of the pattern of a 32-element array with uniform excitation of the modes

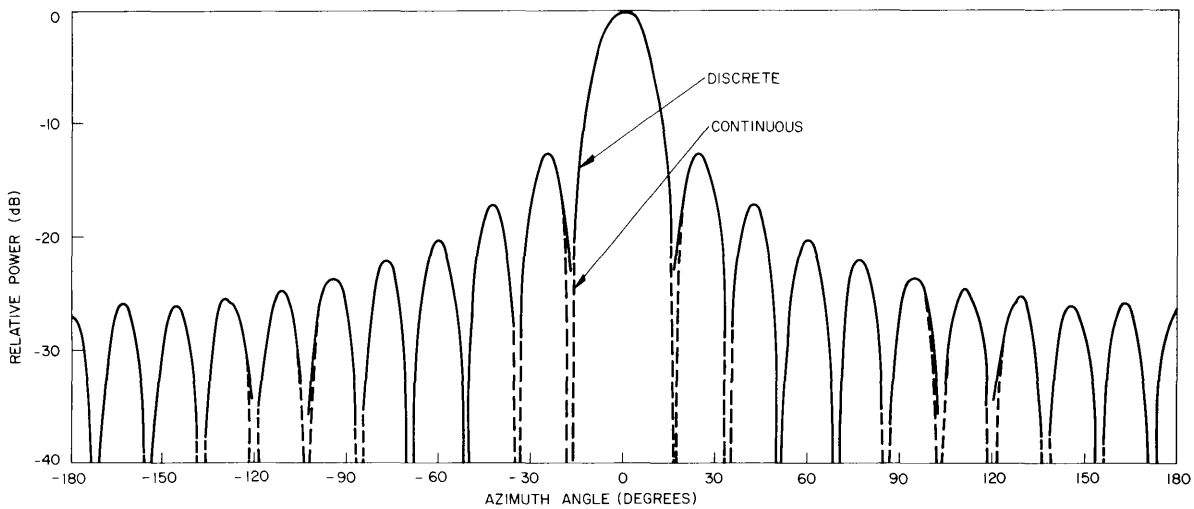

(a) Sum of modes -10 through +10

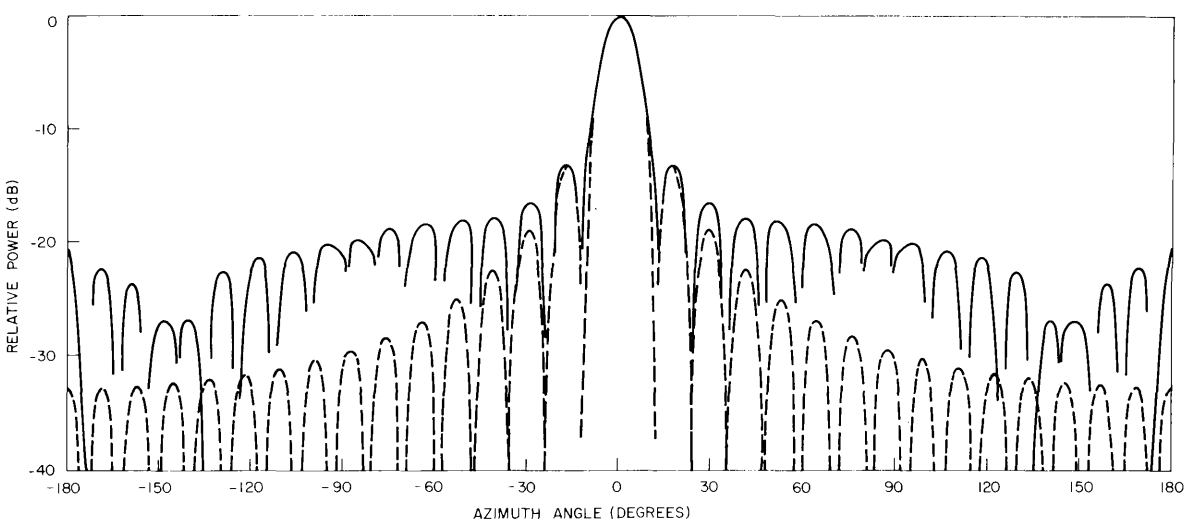

(b) Sum of modes -15 through +15

Fig. 7 - Comparison of the patterns of a 32-element array and of a continuous current sheet, using 21 and then 31 uniformly excited modes

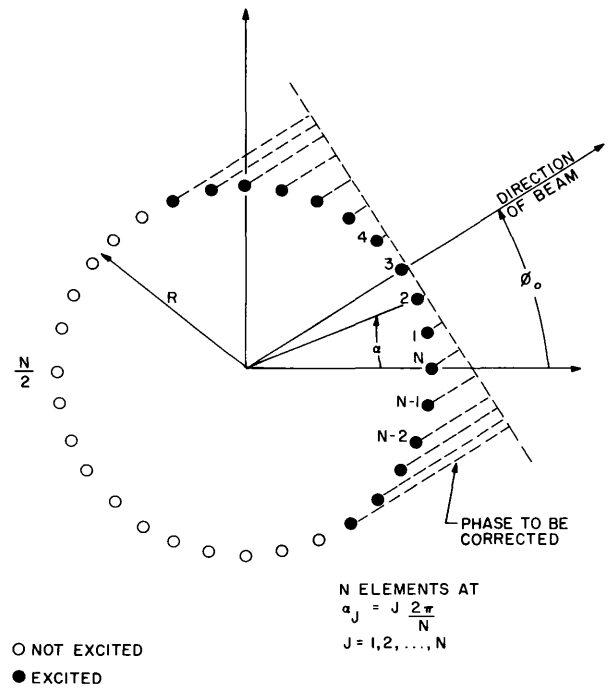

Fig. 8 - Geometry for the cophasal distribution

Table 2
The Current Distribution on a 32-Element Array with Uniformly Excited Modes, Compared with a Cophasal Distribution

Element Number	Power (dB)	Phase (degrees)	Phase Variation from Cophasal	Element Number	Power (dB)	Phase (degrees)	Phase Variation from Cophasal
1	-3.44732	175.48183	11.8	17	-21.95263	179.11611	—
2	-0.05273	-134.29380	13.8	18	-25.74411	10.08901	—
3	-0.45288	-29.86873	6.8	19	-25.95690	115.87377	—
4	-4.12162	96.31795	18.1	20	-19.17377	-68.86822	—
5	-9.23428	-134.74211	8.6	21	-17.13523	129.24006	—
6	-11.60679	-3.78167	33.5	22	-16.15650	-49.15206	—
7	-12.45165	156.25335	—	23	-16.63500	136.38897	—
8	-14.95675	-28.98433	—	24	-14.95675	-28.98430	—
9	-16.63499	136.38895	—	25	-12.45165	156.25339	—
10	-16.15650	-49.15207	—	26	-11.60680	-3.78159	33.5
11	-17.13523	129.24005	—	27	-9.23429	-134.74200	8.6
12	-19.17377	-68.86822	—	28	-4.12162	96.31803	18.1
13	-25.95691	115.87382	—	29	-0.45288	-29.86869	6.8
14	-25.74410	10.08906	—	30	-0.05273	-134.29377	13.8
15	-21.95262	179.11612	—	31	-3.44732	175.48185	11.8
16	-22.16723	8.13703	—	32	0.00000	169.67831	0.0

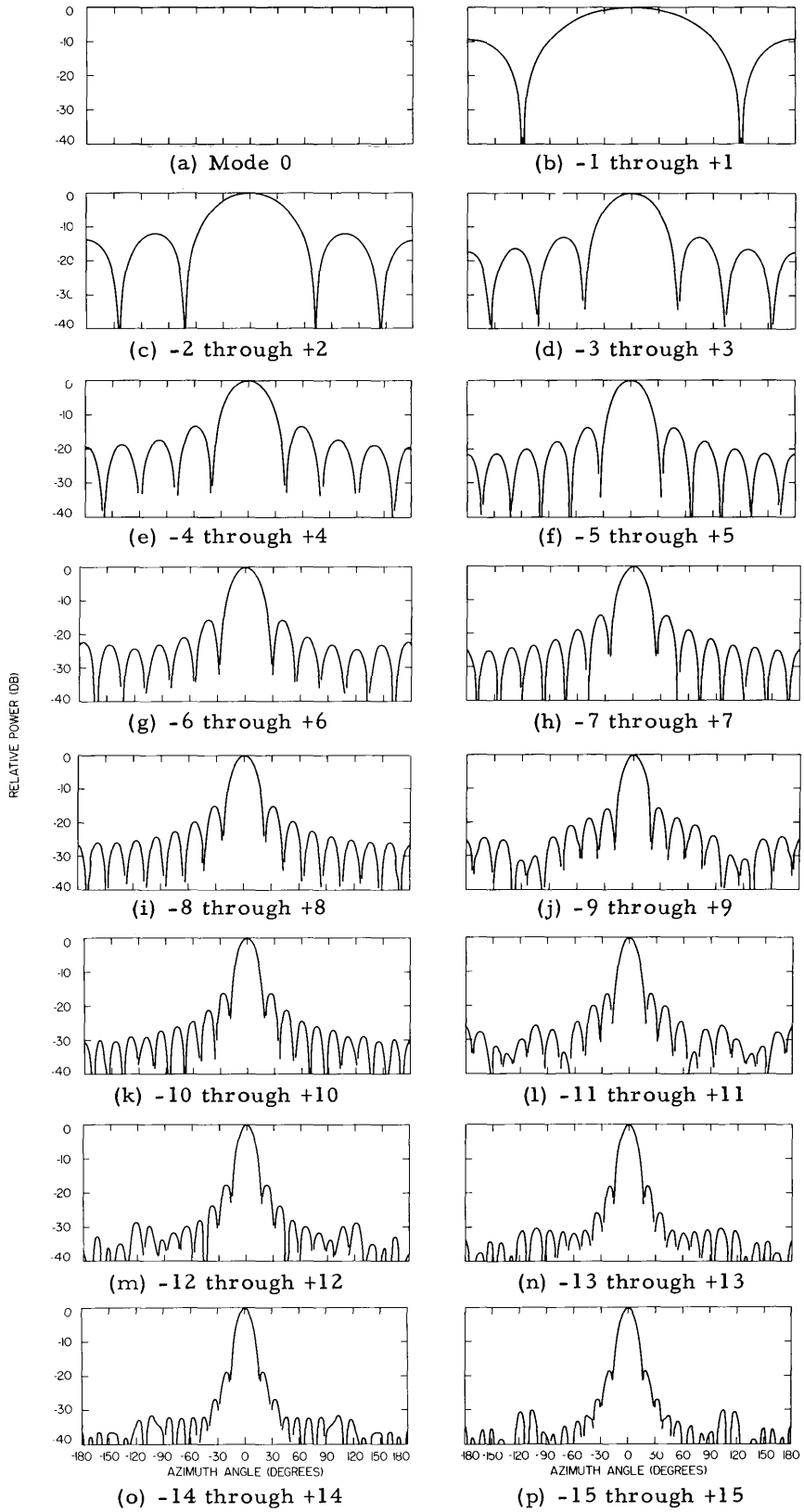

Fig. 9 - Mode-by-mode buildup of the pattern of a 32-element array with cosine amplitude taper on the modes

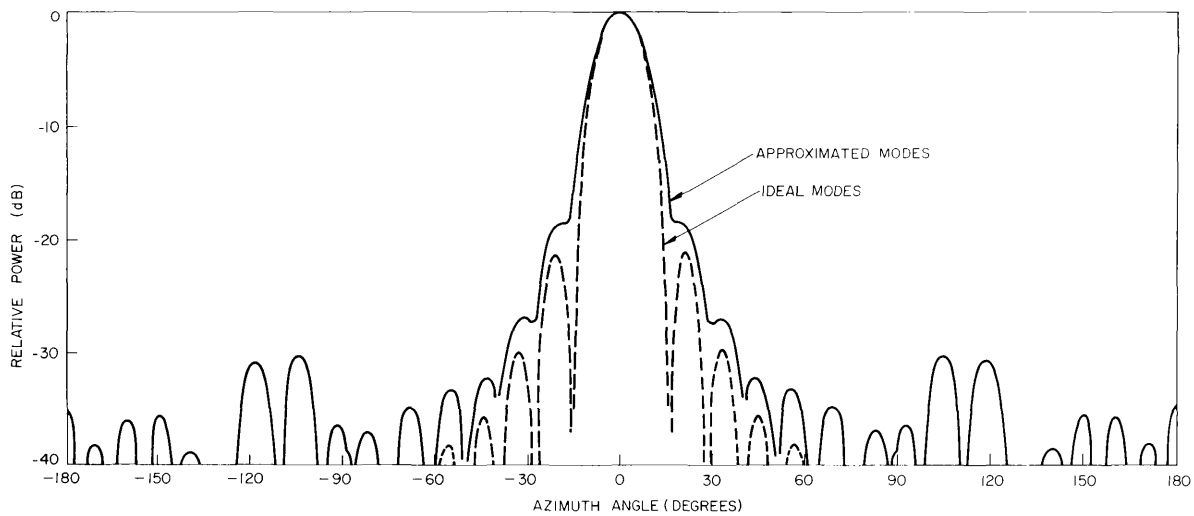

Fig. 10 - Comparison of the patterns of a 32-element array and of a continuous current sheet, using cosine amplitude taper on 31 modes

on the array and the deviation from a cophasal condition are given in Table 3. More than 97% of the total power is radiated from nine elements, and on these elements the currents differ from cophasal by at most 5 degrees.

One of the distributions used in the experimental program was $B_K = \cos^2(\pi K/40)$, which provided a 17-dB taper over the 31 mode inputs. To indicate how much the pattern shape could be expected to change as the beam was scanned, patterns were computed for various beam positions. Figure 11 shows three patterns, one phased so that its peak is in the direction of element 32 ($\phi = 0$), the other two having the same amplitude distribution over the modes but phased to scan the beam one-quarter and one-half, respectively, of the angle between elements. The current distribution on the array for each of the patterns appear in Table 4; the second and third distributions are symmetrical, since only these correspond to patterns symmetrically located with respect to the elements. It may be seen that, at least for this distribution, the pattern changes only slightly as the beam is scanned.

Patterns were also calculated for different element spacings, element patterns, and amplitude distributions, but those shown satisfactorily illustrate the beam formation and scanning and also indicate how the pattern differs from one based on the existence of perfect pattern modes.

SYNTHESIS OF APERTURE DISTRIBUTIONS

It should now be evident that the radiation pattern of a circular array computed on the assumption that the pattern modes are perfect is not the same as that computed from the actual current distribution, and that a certain amount of cut-and-try is involved in determining the number of modes to use and in adjusting the phases of the modes to form a beam in a particular direction. Instead of picking the mode excitations, only to find that the corresponding current distribution results in a poor radiation pattern, it would be preferable first to pick a current distribution having an acceptable pattern and then to find the mode excitations which will give these currents. That this is always possible was discovered by Davies (7) who showed that any prescribed output currents can be

Table 3
The Current Distribution on a 32-Element Array with Cosine Taper on the Modes, Compared with a Cophasal Distribution

Input			Aperture Distribution on the Array			
Mode	Amplitude	Phase (radians)	Element	Power (dB)	Phase (degrees)	Deviation from Cophasal (degrees)
0	1.00000	-2.66400	1	-0.47257	-176.49142	3.1
-1	0.99517	-2.67700	2	-1.75887	-123.19997	2.0
1	0.99517	-2.67700	3	-4.50998	-38.68408	2.2
-2	0.98079	-2.79500	4	-9.18096	72.52077	5.0
2	0.98079	-2.79500	5	-14.80740	-166.42169	—
-3	0.94622	-2.91900	6	-18.44634	-35.00849	—
3	0.94622	-2.91900	7	-21.73024	133.34552	—
-4	0.92388	3.09000	8	-31.54853	-41.41308	—
4	0.92388	3.09000	9	-32.89055	75.26568	—
-5	0.88192	2.83900	10	-29.02351	-71.29683	—
5	0.88192	2.83900	11	-30.86602	113.83807	—
-6	0.83147	2.51800	12	-28.29847	-112.19534	—
6	0.83147	2.51800	13	-32.42267	5.40598	—
-7	0.77023	2.01400	14	-30.31264	91.12548	—
7	0.77023	2.01400	15	-33.26910	-158.42240	—
-8	0.70711	1.60500	16	-33.21392	70.90724	—
8	0.70711	1.60500	17	-33.26910	-158.42240	—
-9	0.63776	1.09500	18	-30.31264	91.12548	—
9	0.63776	1.09500	19	-32.42267	5.40598	—
-10	0.55557	0.27500	20	-28.29847	-112.19534	—
10	0.55557	0.27500	21	-30.86602	113.83807	—
-11	0.47140	-0.39200	22	-29.02351	-71.29683	—
11	0.47140	-0.39200	23	-32.89055	75.26568	—
-12	0.38268	-0.92100	24	-31.54853	-41.41308	—
12	0.38268	-0.92100	25	-21.73024	133.34552	—
-13	0.32350	-1.90400	26	-18.44634	-35.00849	—
13	0.32350	-1.90400	27	-14.80740	-166.42169	—
-14	0.19509	3.12400	28	-9.18096	72.52077	5.0
14	0.19509	3.12400	29	-4.50998	-38.68408	2.2
-15	0.09800	2.73100	30	-1.75887	-123.19997	2.0
15	0.09800	2.73100	31	-0.47257	-176.49142	3.1
			32	0.00000	168.95482	0.0

achieved with a Butler matrix by properly exciting the matrix inputs. To demonstrate this, consider a Butler matrix with outputs labeled $J = 1, 2, \ldots, N$ and the inputs labeled $K = 1, 2, \ldots, N$, with the property that a current into input K results in currents

$$\frac{1}{\sqrt{N}} e^{jKJ(2\pi/N)}$$

on the output ports. This is the definition used previously, except that the inputs have been relabeled with $K = 1, 2, \ldots, N$ now corresponding to modes $1, 2, \ldots, N/2, \ldots, -1, 0$, respectively. Note that all the modes, when fed in phase, have the same phase at the Nth output terminal. When this is true the matrix is bilateral; i.e., if the roles of the inputs and the outputs are reversed, the matrix is again a Butler matrix having a zero

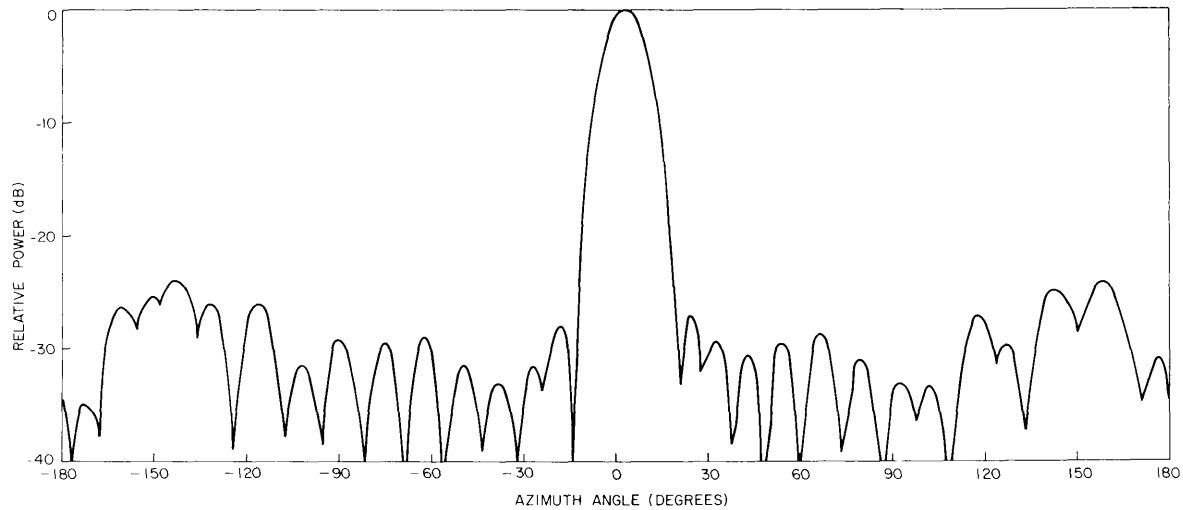

(a) One-quarter way between dipoles 32 and 1

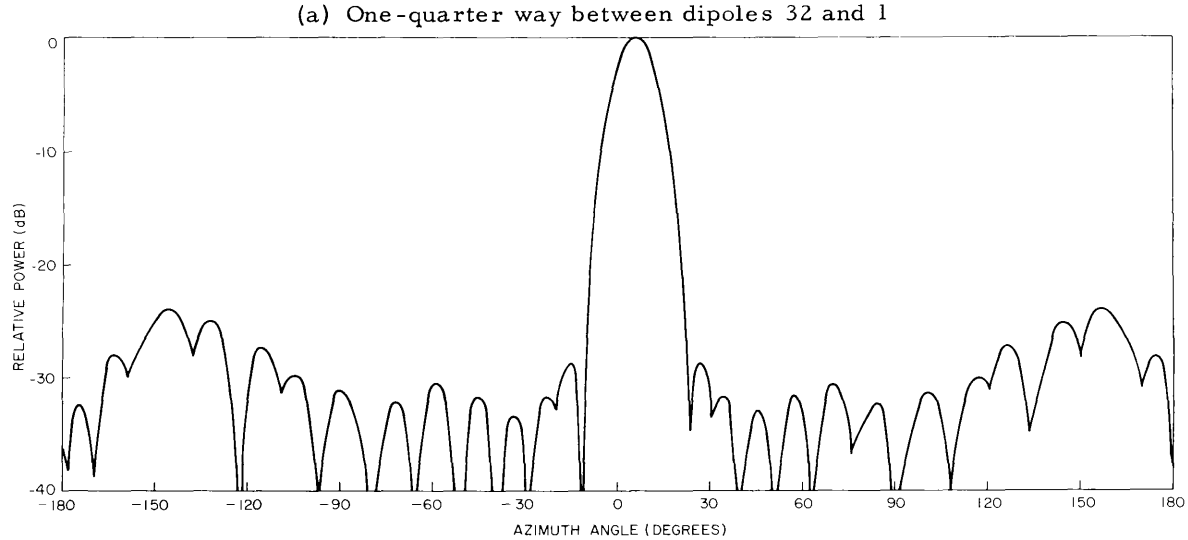

(b) Midway between dipoles 32 and 1

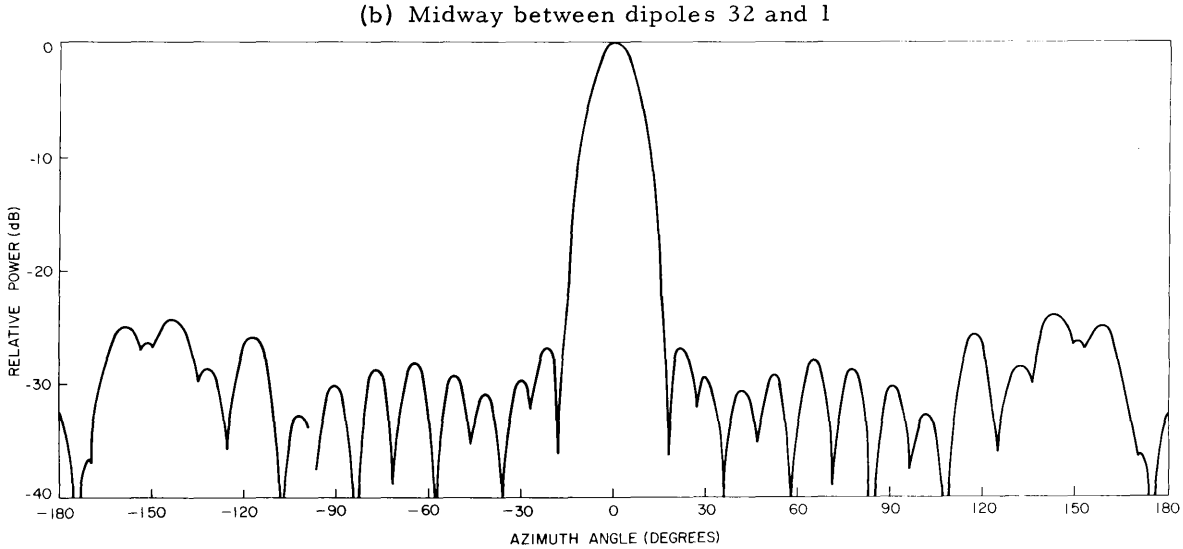

(c) On dipole 32

Fig. 11 - Patterns for beams at 0°, 2.813°, and 5.625°. The amplitude taper on the modes is $B_K = \cos^2(\pi K/40)$, with $K = 0, \pm 1, \pm 2, \ldots, \pm 15$.

Table 4
Aperture Distribution

Asymmetric Case (a)				Symmetric Case (b)				Symmetric Case (c)			
J	Power (dB)	Phase (degrees)	Relative Power	J	Power (dB)	Phase (degrees)	Relative Power	J	Power (dB)	Phase (degrees)	Relative Power
1	-0.21668	176.62222	0.95133	1	-0.00000	171.99979	1.00000	1	-0.44343	-176.60862	0.90294
2	-1.55109	-141.90281	0.69967	2	-0.99395	-156.00899	0.79544	2	-2.11568	-125.20641	0.61437
3	-3.77393	-65.54656	0.41938	3	-3.06736	-86.15058	0.49347	3	-4.73247	-44.38657	0.33632
4	-8.96522	38.95468	0.12690	4	-7.62366	6.54675	0.17284	4	-9.52727	70.76172	0.11150
5	-14.39432	150.57976	0.03636	5	-11.45312	121.78994	0.07156	5	-17.48372	-163.78746	0.01785
6	-16.71394	-62.86015	0.02131	6	-15.85444	-82.85757	0.02598	6	-20.31012	-41.88725	0.00931
7	-20.83982	119.71317	0.00824	7	-24.44876	94.86337	0.00359	7	-20.71442	131.29208	0.00848
8	-31.40056	29.70634	0.00072	8	-31.14171	122.73945	0.00077	8	-25.51536	17.35010	0.00281
9	-32.25528	4.63284	0.00059	9	-25.86347	22.59884	0.00259	9	-30.92661	-84.04295	0.00081
10	-21.72481	-91.70139	0.00672	10	-21.57459	-96.29391	0.00696	10	-24.50283	-87.60305	0.00355
11	-25.82403	148.82783	0.00262	11	-33.69180	154.78219	0.00043	11	-22.77846	161.60114	0.00527
12	-22.82111	-153.00851	0.00522	12	-21.20791	-166.18353	0.00757	12	-28.15539	-143.27151	0.00153
13	-18.76618	59.67982	0.01329	13	-23.48150	54.29705	0.00449	13	-16.76397	65.15051	0.02107
14	-18.39255	90.06239	0.01448	14	-16.93887	79.19901	0.02024	14	-19.81080	103.98944	0.01045
15	-21.22390	133.47058	0.00754	15	-20.84027	127.76109	0.00824	15	-21.89253	137.51160	0.00647
16	-25.30403	157.70873	0.00295	16	-24.17335	149.80169	0.00383	16	-25.71077	161.33603	0.00268
17	-22.94357	142.51320	0.00508	17	-24.17334	149.80167	0.00383	17	-21.89253	137.51159	0.00647
18	-20.60362	117.86860	0.00870	18	-20.84027	127.76107	0.00824	18	-19.81079	103.98941	0.01045
19	-16.31634	71.30738	0.02335	19	-16.93887	79.19899	0.02024	19	-16.76398	65.15050	0.02107
20	-39.67240	52.94398	0.00011	20	-23.48152	54.29704	0.00449	20	-28.15537	-143.27152	0.00153
21	-21.42659	177.96982	0.00720	21	-21.20791	-166.18356	0.00757	21	-22.77846	161.60111	0.00527
22	-32.19092	-94.49640	0.00060	22	-33.69183	154.78227	0.00043	22	-24.50282	-87.60306	0.00355
23	-24.20390	-98.25608	0.00380	23	-21.57459	-96.29391	0.00696	23	-30.92663	-84.04288	0.00081
24	-24.12936	20.44488	0.00386	24	-25.86346	22.59884	0.00259	24	-25.51536	17.35010	0.00281
25	-23.58973	136.81066	0.00438	25	-31.14169	122.73954	0.00077	25	-20.71442	131.29206	0.00848
26	-27.46216	9.66008	0.00179	26	-24.44877	94.86329	0.00359	26	-20.31011	-41.88730	0.00931
27	-17.09603	-113.17053	0.01952	27	-15.85444	-82.85761	0.02598	27	-17.48371	-163.78756	0.01785
28	-10.04857	97.60342	0.09889	28	-11.45312	121.78989	0.07156	28	-9.52727	70.76167	0.11150
29	-6.07377	-21.15001	0.24696	29	-7.62366	6.54669	0.17284	29	-4.73247	-44.38661	0.33632
30	-2.62493	-106.31989	0.54639	30	-3.06736	-86.15062	0.49347	30	-2.11568	-125.20645	0.61437
31	-0.69653	-167.53290	0.85182	31	-0.99395	-156.00901	0.79544	31	-0.44343	-176.60863	0.90294
32	0.00000	169.33749	1.00000	32	0.00000	171.99979	1.00000	32	0.00000	168.47203	1.00000

mode. To show this, assume that the N inputs are excited simultaneously with currents $e^{jKM(2\pi/N)}$, where M is an integer and $K = 1, 2, \ldots, N$. The output currents are then given by

$$A_J e^{j\psi_J} = \sum_{K=1}^{N} e^{jK(M+J)(2\pi/N)} = e^{j(M+J)(\pi/N)} e^{j(M+J)\pi} \frac{\sin[(M+J)\pi]}{\sin\left[(M+J)\frac{\pi}{N}\right]}, \tag{21}$$

which vanishes unless $J = N - M$. Therefore, all the power must exit from the $(N-M)$th terminal. Then, by reciprocity, if the Mth output port is excited, currents corresponding to the Mth mode appear on the N input terminals and the matrix is bilateral.

If the prescribed currents $A_J e^{j\psi_J}$, where $J = 1, 2, \ldots, N$ are to be set up on the array, the N currents that must be applied to the inputs of the matrix are

$$B_K e^{j\beta_K} = \sum_{J=1}^{N} A_J e^{j\psi_J} e^{-jKJ(2\pi/N)} . \tag{22}$$

These currents are conjugate to those that would appear at the inputs if currents $A_J e^{-j\psi_J}$ were fed into the outputs of the matrix. The correctness of Eq. (22) may be verified by

substitution into Eq. (17). As has been shown previously, since the matrix has a zero mode (looking from input to output), the current distribution that has been set up can be moved, intact, M elements around the array by holding the amplitudes B_K of the input currents fixed but changing their phases by applying a linear phase progression with a mode-to-mode phase difference of $M(2\pi/N)$.

It might seem unnecessarily restrictive to assume that the Butler matrix be bilateral and have a zero mode, but it may be shown that the matrix must be of this type if it is to be used to commute the currents around a circular array using phase shifters alone. If a matrix not satisfying these conditions is used, it is found that fixed phase shifts must be added at the inputs and/or at the outputs, and when these are lumped with the matrix, the resultant network is a bilateral, zero-mode Butler matrix.

It has been shown that the current distribution and the radiation pattern of a multimode array are invariant (aside from rotation) if the beam is scanned in steps equal to the angle between elements. For any other angle of scan, the current distribution will be changed. If, for example, all inputs are fed in phase with equal amplitudes, only element N will be excited. If the linear phase progression $e^{-jK(2\pi/N)}$ is then applied to the inputs, the excitation is switched to element 1. If, however, the linear phase progression were only half this (i.e., $e^{-jK(\pi/N)}$), two elements, N and 1, would be strongly excited, but there would be currents on all the elements of the array. As a practical example, consider a 32-element array with a cophasal distribution on the 14-element sector which includes elements 26 through 7. The desired amplitude distribution is $\cos\{[K-(1/2)]\pi/16\}$, which is symmetrical about a point midway between elements 32 and 1, and the elements are to be phase to form a beam in this direction. All other elements are to be inert. To show how the current distribution varies as the beam is scanned in small steps, the input currents required to achieve this distribution are first determined from Eq. (22), then their phases are changed to scan the pattern and the new distribution on the array is computed from Eq. (17). Table 5 gives the original distribution, phased for a peak at $\phi = 5.625°$, and the corresponding input currents to the Butler matrix. Also in Table 5 is the distribution on the array when the beam is scanned to 11.25° (the direction of element 1) and the distribution when the beam is scanned to the angle midway between the first two. It is seen that, for the scanned beams, the currents are no longer confined to a sector; all elements are illuminated, with those on the rear of the array about 30 dB down. The stronger currents are on 15 or 16 elements, and over this sector there are only minor amplitude ripples with the currents differing from the cophasal condition by about 20 degrees. The two scanned patterns (Fig. 12) do not differ significantly from the original one. Their beamwidths, near-in sidelobes, and the general level of their far-out lobes are comparable. If the distribution had been designed for very low sidelobes, it is likely that the pattern changes would have been more significant.

EXPERIMENTAL PROGRAM

The circular arrays used in the experimental program had either 16 or 32 elements and were operated at 900 MHz. Various radiating elements were used: dipoles, short back-fire elements, and Yagis (the latter two to reduce the elevation beamwidth without increasing the height of the antenna), but the only array that will be described is a 32-element array of slot-fed dipoles, vertically polarized, spaced 0.5λ apart and 0.25λ from a conducting cylinder. This antenna is shown in Fig. 13, and the associated beamforming and scanning network is shown in Fig. 14. The Butler matrix was supplied by the Advanced Development Laboratories, Nashua, New Hampshire, and consisted of two 16-element matrices plus the proper interconnecting networks to form a 32-element matrix. Since 3-dB quadrature couplers were used in the matrix, it had no zero mode; therefore, the coaxial cables connecting the matrix to the dipoles had to be cut to the proper lengths to correct for this. Corporate structures made in triplate line were used to establish the various amplitude distributions over the inputs to the Butler matrix.

Table 5
Cophasal Distribution for the Beam at 5.625 Degrees with Required Input Currents and the Current Distribution on the Array for Beams Scanned to 8.438 Degrees and 11.25 Degrees

Input to Modes			Beam Position											
			Between Elements 32 and 1				On Element 1				One-quarter Way Between Elements 1 and 32			
Mode	Amplitude	Phase (rad)	Element	dB	Phase (deg)	Cophasal Deviations (deg)	Element	dB	Phase (deg)	Cophasal Deviations (deg)	Element	dB	Phase (deg)	Cophasal Deviations (deg)
-15	0.05014	-2.98853	1	0.00000	4.41432	0.0	1	0.00000	1.30606	1.3	1	0.00000	1.98974	0.1
-14	0.16982	-2.80781	2	-0.51926	39.47402	0.0	2	-2.01691	17.80973	0.2	2	-1.64249	28.35642	0.6
-13	0.31358	-2.60148	3	-1.43457	108.24662	0.0	3	-1.10324	64.83482	5.0	3	-1.45862	83.40640	5.6
-12	0.43767	-2.37450	4	-2.84185	-151.91152	0.0	4	-2.07344	160.91891	6.4	4	-2.17622	-176.63541	0.1
-11	0.51999	-2.09735	5	-4.93675	-24.83651	0.0	5	-5.79880	-80.13033	11.4	5	-5.09892	-48.91991	8.0
-10	0.59752	-1.76797	6	-8.17489	124.58780	0.0	6	-10.95202	43.41646	3.0	6	-10.31497	94.83752	5.0
-9	0.68904	-1.42198	7	-14.02687	-69.38130	0.0	7	-13.44224	164.97679	10.9	7	-18.95701	-132.54333	26.00
-8	0.73786	-1.03866	8	-110.95878	9.40060	—	8	-13.49060	-44.26421	62.2	8	-18.54252	-39.69405	—
-7	0.70416	-0.53875	9	-110.29151	-127.37128	—	9	-19.78507	147.62327	—	9	-23.49840	149.10857	—
-6	0.63277	0.07777	10	-108.42737	-80.12002	—	10	-22.97828	-27.73955	—	10	-26.36628	-26.97267	—
-5	0.49759	0.68746	11	-112.01176	103.52423	—	11	-25.16028	154.81247	—	11	-28.37765	155.27371	—
-4	0.23592	1.46408	12	-111.17657	-75.03709	—	12	-26.75804	-23.60801	—	12	-29.86092	-23.31109	—
-3	0.17912	-2.74105	13	-107.88319	-119.27306	—	13	-27.94438	157.42682	—	13	-30.96016	157.62730	—
-2	0.25706	-1.78156	14	-117.77163	34.95047	—	14	-28.80676	-21.90153	—	14	-31.75041	-21.77114	—
-1	0.25264	-0.54328	15	-112.87704	65.89978	—	15	-29.39541	158.52920	—	15	-32.27577	158.60405	—
0	0.41310	0.25664	16	-117.61885	-131.95122	—	16	-29.73847	-21.22499	—	16	-32.56037	-21.19276	—
1	0.41310	0.35481	17	-118.16084	-136.67705	—	17	-29.85107	158.85470	—	17	-32.61636	158.85068	—
2	0.25264	-0.24785	18	-111.86473	60.67050	—	18	-29.73843	-21.22460	—	18	-32.44693	-21.26605	—
3	0.25706	-1.29069	19	-122.53436	43.74770	—	19	-29.39536	158.52921	—	19	-32.04448	158.44071	—
4	0.17912	-2.05383	20	-107.81624	-112.96098	—	20	-28.80673	-21.90223	—	20	-31.39070	-22.04947	—
5	0.23592	2.34765	21	-114.45265	-75.31601	—	21	-27.94435	157.42611	—	21	-30.45327	157.20708	—
6	0.49759	1.76738	22	-116.41499	94.23270	—	22	-26.75802	-23.60789	—	22	-29.17439	-23.93888	—
7	0.63277	1.35404	23	-109.30689	-95.61509	—	23	-25.16029	154.81323	—	23	-27.45203	154.29411	—
8	0.70416	0.93386	24	-113.19501	-108.60654	—	24	-22.97834	-27.73904	—	24	-25.07565	-28.62743	—
9	0.73786	0.63030	25	-113.92446	8.94868	—	25	-19.78514	147.62316	—	25	-21.47069	145.78916	—
10	0.68904	0.44333	26	-14.02684	-69.38122	0.0	26	-13.49063	-44.26440	62.2	26	-12.17991	-51.94113	—
11	0.59752	0.29369	27	-8.17489	124.58789	0.0	27	-13.44226	164.97683	10.9	27	-9.45066	143.16679	28.0
12	0.51999	0.16066	28	-4.93675	-24.83631	0.0	28	-10.95202	43.41665	3.0	28	-7.73339	1.07559	13.00
13	0.43767	0.07986	29	-2.84186	-151.91129	0.0	29	-5.79880	-80.13017	11.4	29	-5.12229	-118.84582	0.2
14	0.31358	0.04923	30	-1.43458	108.24684	0.0	30	-2.07344	160.91905	6.4	30	-2.07351	135.92040	5.0
15	0.16982	0.03925	31	-0.51925	39.47413	0.0	31	-1.10324	64.83485	5.0	31	-0.76244	51.05834	4.0
16	0.05014	0.05488	32	-0.00002	4.41439	0.0	32	-2.01692	17.80984	0.2	32	-1.35198	9.49976	3.5

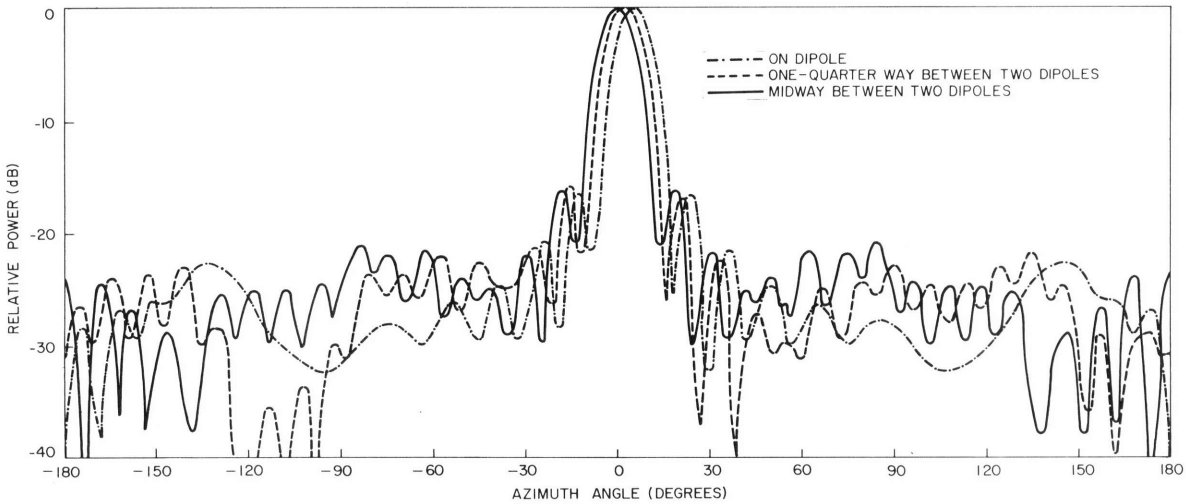

Fig. 12 - Pattern of the 32-element array with a synthesized cophasal distribution and patterns when scanned to 8.44° and 11.25°

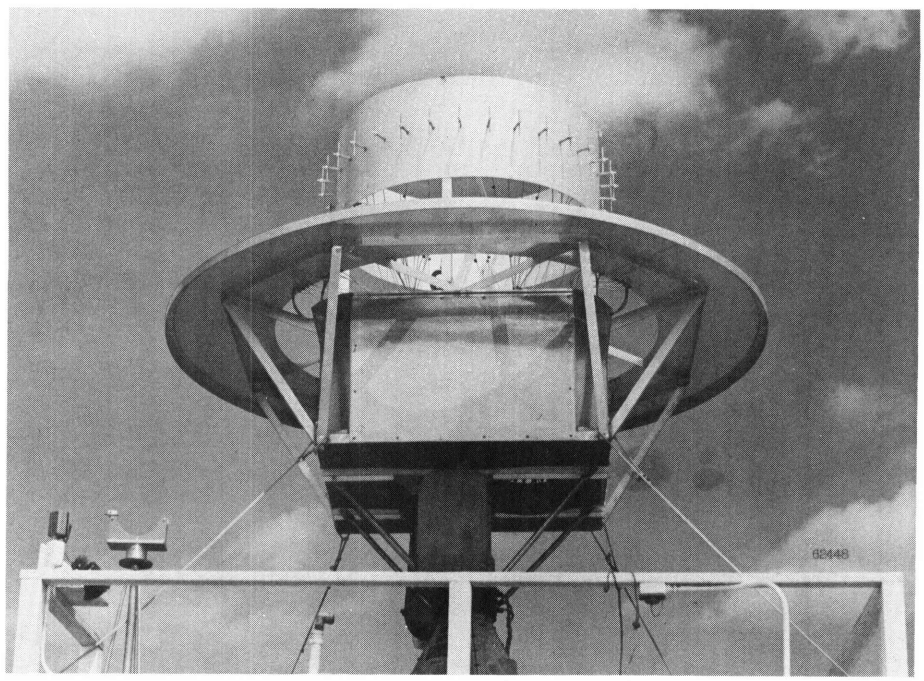

Fig. 13 - Circular array of 32 dipoles
($\lambda/2$ spacing, 900 MHz)

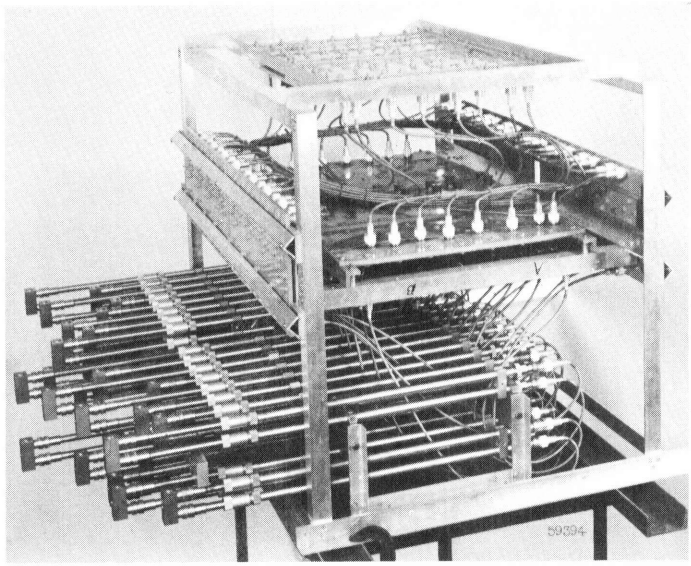

Fig. 14 - Beam-forming and scanning network for the 32-dipole array

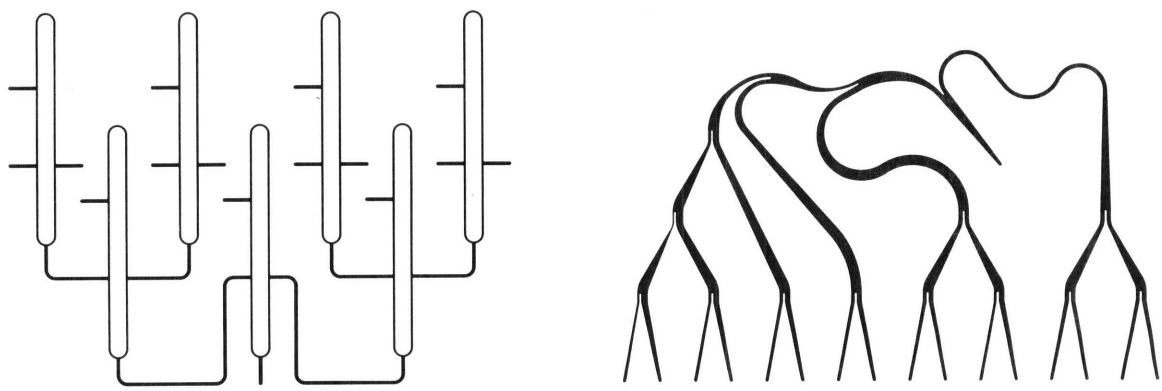

(a) Uniform output (b) Tapered distribution

Fig. 15 - Printed circuit corporate structures for feeding the Butler matrices

Figure 15 shows the center conductors of two 16-element corporate structures — one for a uniform distribution, the other for a cosine-squared distribution on a 17-dB pedestal. Other amplitude tapers were used; none however were designed following the synthesis technique described in the preceding section. In the lines connecting the corporate structure to the Butler matrix were variable phase shifters (General Radio Type 874-LTL Trombones), with a maximum pathlength variation of one wavelength, which were used first to adjust the relative phases of the modes to form a beam in a desired direction and then to scan the pattern.

The measured mode patterns for this array (Fig. 16) do not compare favorably with the computed patterns in Fig. 5. The deviations are attributable primarily to phase and amplitude errors in the matrix. All the current modes were fed so as to have the same phase at element 32, and the relative phases of the pattern modes were determined by

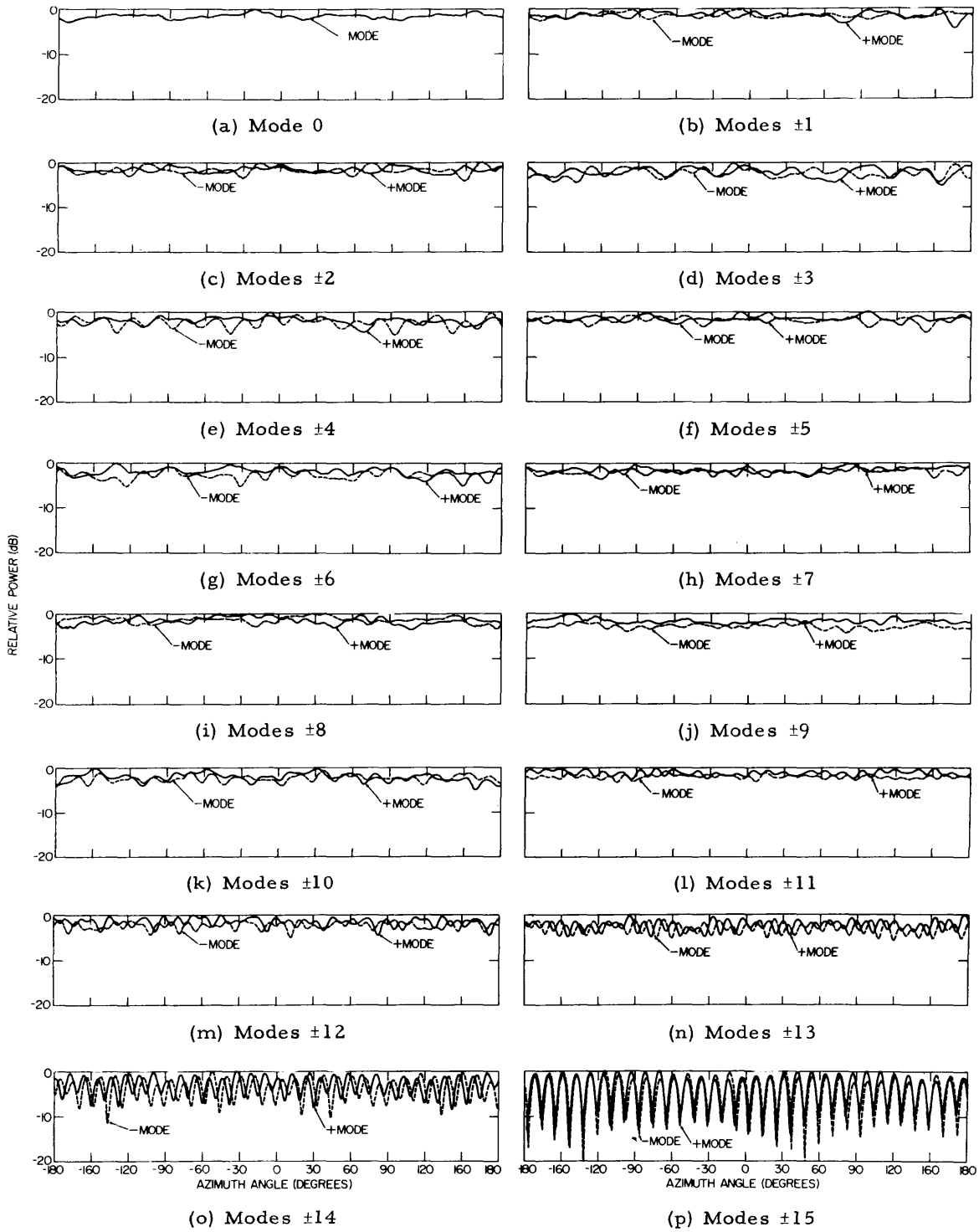

Fig. 16 - Measured mode patterns for the 32-dipole array

comparing the phase of each mode with that of the zero mode in the far field at $\phi = 0$. This was done by feeding the two modes from the difference arms of a rat-race hybrid, then adjusting the phase shifter at the input port of the mode being phased until the far-field pattern showed a minimum in the specified direction. A final 180-degree adjustment in the phase of the zero mode then put all the pattern modes in phase at $\phi = 0$. This procedure is most accurate when the two signals have equal amplitude; when a minimum of a mode pattern happened to lie in the direction in which the modes were being phased, the comparison was made at a slightly different angle, and the error resulting from this was then accounted for by adding an amount computed from the theoretical phase distribution for that mode.

Figure 17 shows the pattern of the array when a corporate structure was used providing currents of equal amplitude to all the mode inputs but number 16. For comparison, the corresponding calculated pattern (from Fig. 7) is shown solid. The two patterns agree reasonably well; both have beamwidths of about 10 degrees, the measured first sidelobes are 1.5 dB higher than those calculated, and the general level of the far-out sidelobes is about 21 dB down for both.

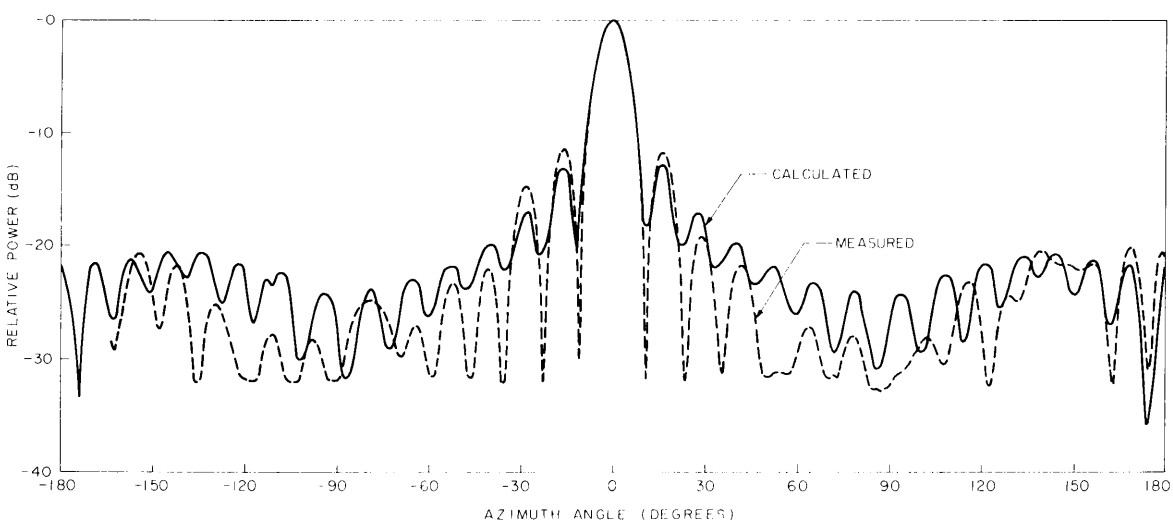

Fig. 17 - Measured and calculated patterns of the 32-element array with uniformly excited modes

The next series of patterns was taken with a tapered amplitude distribution over the modes. Thirty-one modes were fed from a 16-element corporate structure by dividing the outputs with tees. This resulted in a stepped distribution (since pairs of adjacent modes had equal amplitudes) with a 17-dB taper. The mode-by-mode buildup of the pattern is shown in Fig. 18, and Fig. 19 compares the final pattern, which includes all but the 16th mode, with the corresponding calculated pattern. The measured beamwidth (11.5 degrees) and the first sidelobe (19 dB down) agree well with those calculated, but the level of the far-out lobes was somewhat worse than for the calculated pattern. The beam was then scanned by operating the phase shifters, and some of the patterns are shown in Fig. 20. It was found that the beamwidth and sidelobe level changed only slightly, and the gain varied by about 1 dB as the beam was scanned.

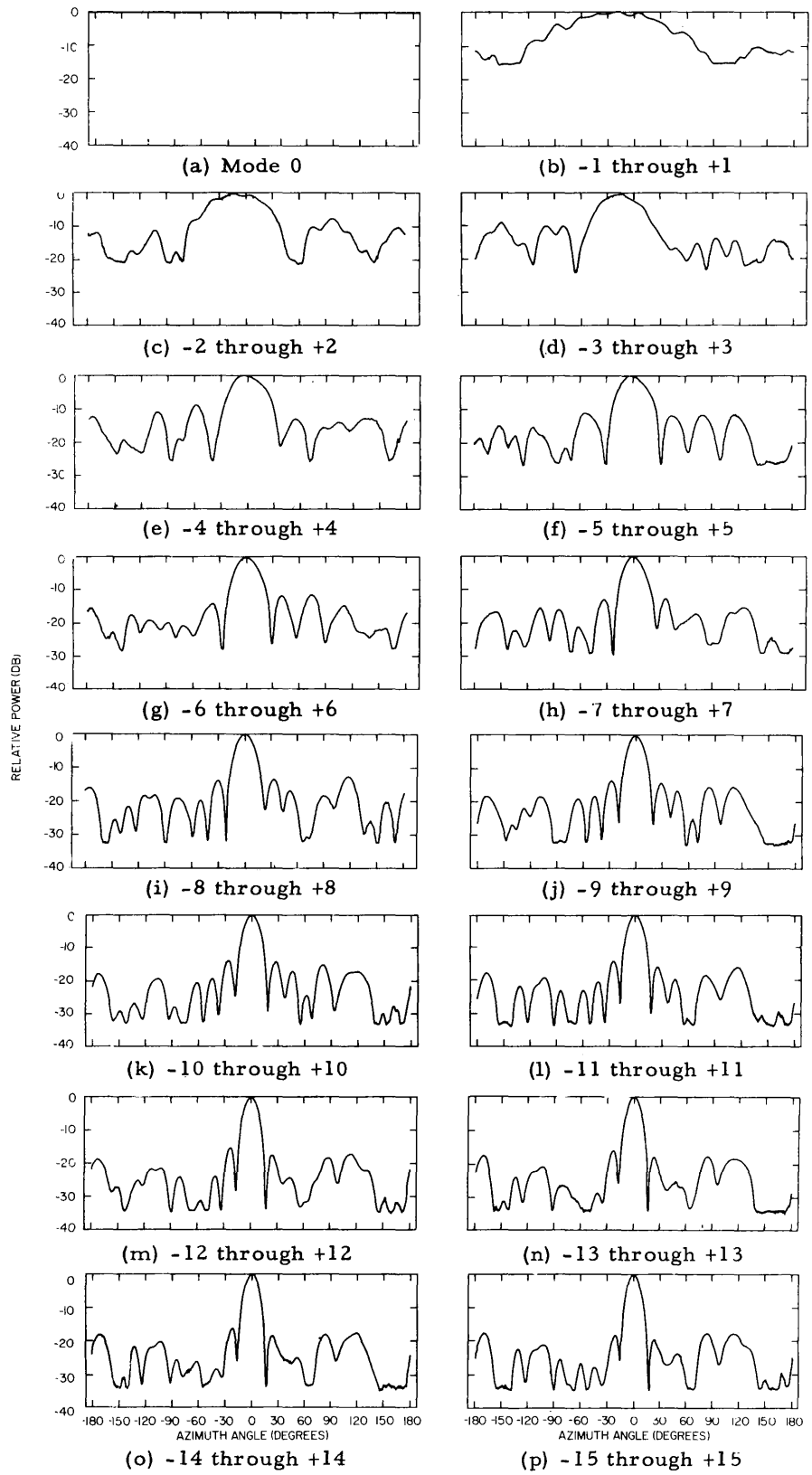

Fig. 18 - Measured mode-by-mode buildup of the pattern with a tapered, stepped distribution on the modes

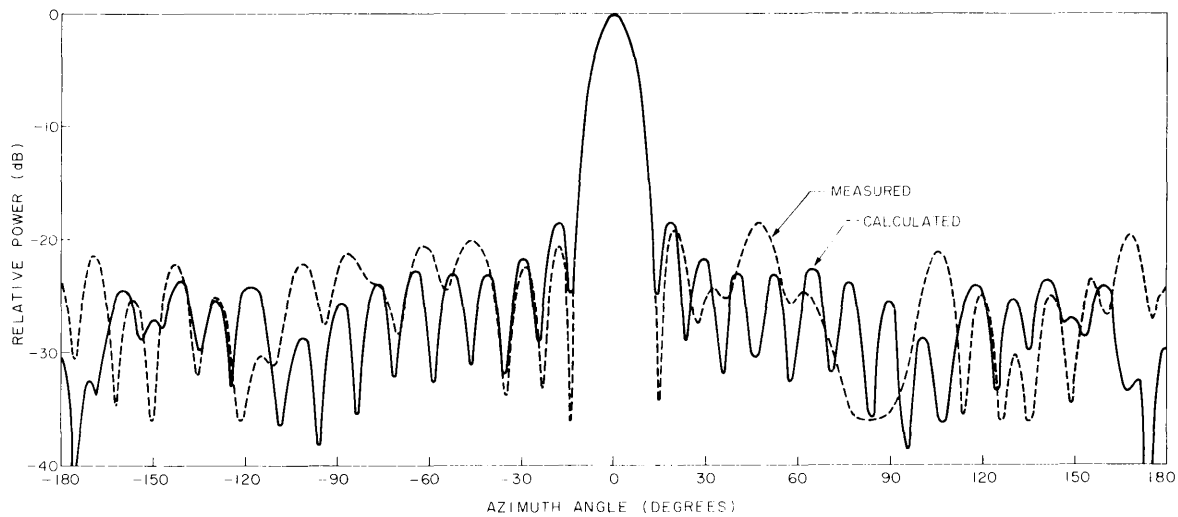

Fig. 19 - Measured and calculated patterns of the 32-element array with a tapered, stepped distribution on the modes

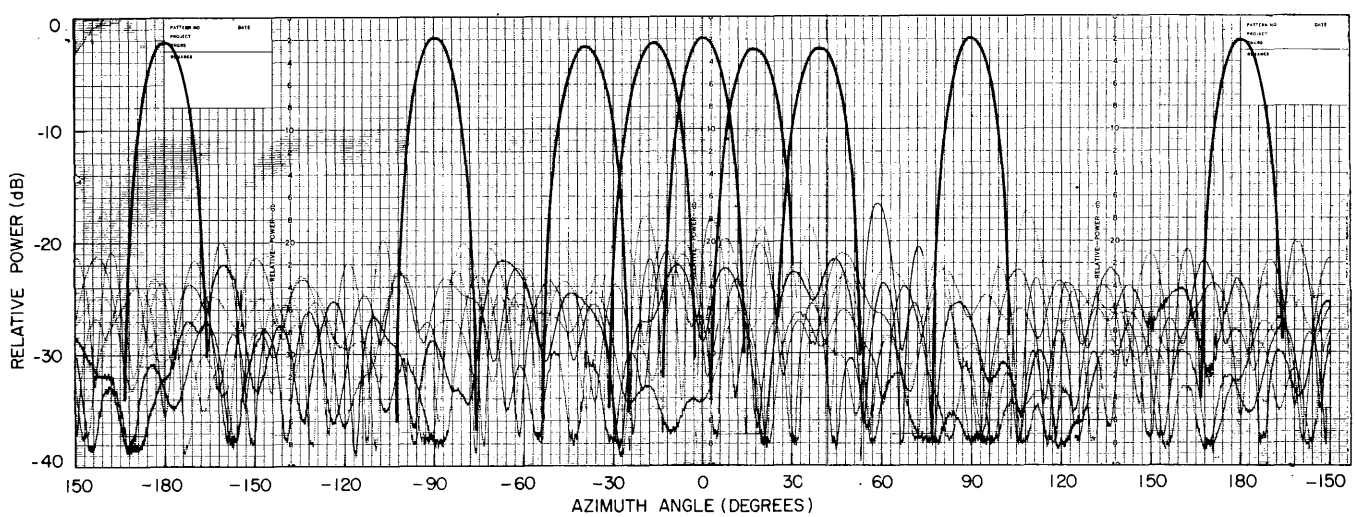

Fig. 20 - Scanned patterns for the 32-element array with a tapered, stepped distribution on the modes

CONCLUSIONS

It has been shown that a Butler matrix can be used to feed a circular array to form a narrow pattern which can be scanned through 360 degrees in azimuth by the operation of phase shifters alone. One explanation of this, based on the assumption that the radiation pattern could be written as the sum of a finite number of uniform pattern modes, was found to work only qualitatively in that it could not be used to predict the structure of the sidelobes. A 32-element array of dipoles was used to demonstrate experimentally how a beam was formed by superposition of the pattern modes (even though imperfect) and how the scanning was performed. Finally, the synthesis procedure of Davies was described, and, as an example, the inputs to the Butler matrix required to achieve a prescribed co-phasal sector distribution on the array were determined and the changes in the current distribution for other beam positions were shown.

ACKNOWLEDGMENTS

The author acknowledges the help given by Mr. Russel H. Brown through numerous discussions and consultations, and the contributions of Mr. Fred W. Lashway and Mr. Rudolf J. Wiegand who helped with the mechanical design and the measurement program. In addition, the author expresses his gratitude to Mr. Joseph Tyszkiewicz of the Naval Air Systems Command, who sponsored and supported this work.

REFERENCES

1. Chadwick, G.G., and Glass, J.C., "Investigation of a Multiple Beam Scanning Circular Array," Scientific Report 1 to Air Force Cambridge Research Laboratories, Contract AF19(628)367, Dec. 31, 1962

2. LePage, W.R., Roys, C.S., and Seely, S., "Radiation from Circular Current Sheets," IRE Proc. 38:1069-1072 (1950)

3. Honey, R.C., and Jones, E.M.T., "A Versatile Multiport Biconical Antenna," IRE Proc. 45:1374-1383 (1957)

4. Schell, A.C., and Bouche, E.L., "A Concentric Loop Array," IRE WESCON Convention Record, Vol. 2, Pt. 1, Aug. 1958, pp. 212-215

5. Clasen, C.P., Rankin, J.B., and Woodward, O.M., Jr., "A Radial-Waveguide Antenna and Multiple Amplifier System for Electronic Scanning," RCA Review 22(No. 3):543-554 (1961)

6. Butler, J., and Lowe, R., "Beam-Forming Matrix Simplifies Design of Electronically Scanned Antennas," Electronic Design, Apr. 1961, p. 170

7. Davies, D.E.N., "A Transformation Between the Phasing Techniques Required for Linear and Circular Aerial Arrays," Proc. Inst. Elec. Engrs. (London) 112(No. 11): 2041-2045 (1965)

This page intentionally left blank.

Security Classification

DOCUMENT CONTROL DATA - R & D

(Security classification of title, body of abstract and indexing annotation must be entered when the overall report is classified)

1. ORIGINATING ACTIVITY *(Corporate author)* Naval Research Laboratory Washington, D.C. 20390	2a. REPORT SECURITY CLASSIFICATION Unclassified 2b. GROUP

3. REPORT TITLE

A MATRIX-FED CIRCULAR ARRAY FOR CONTINUOUS SCANNING

4. DESCRIPTIVE NOTES *(Type of report and inclusive dates)*

An interim report on one phase of the problem; work on other phases continues.

5. AUTHOR(S) *(First name, middle initial, last name)*

B. Sheleg

6. REPORT DATE April 2, 1968	7a. TOTAL NO. OF PAGES 32	7b. NO. OF REFS 7
8a. CONTRACT OR GRANT NO. NRL Problem R08-38 b. PROJECT NO. A36533818/6521/F001-02-02 c. d.	9a. ORIGINATOR'S REPORT NUMBER(S) NRL Report 6696 9b. OTHER REPORT NO(S) *(Any other numbers that may be assigned this report)*	

10. DISTRIBUTION STATEMENT

This document has been approved for public release and sale; its distribution is unlimited.

11. SUPPLEMENTARY NOTES	12. SPONSORING MILITARY ACTIVITY Department of the Navy (Naval Air Systems Command), Washington, D.C. 20360

13. ABSTRACT

If the radiators of a circular array are connected to the outputs of a Butler matrix, a focused radiation pattern can be formed by establishing the proper current distribution on the inputs of the Butler matrix. Further, if the amplitudes of the input currents are held fixed, the pattern can be scanned through 360 degrees in azimuth by the operation of phase shifters alone, just as the pattern of a linear array is scanned by varying the phases of the element currents. One explanation of this is based on the assumption that the pattern can be written as the sum of a finite number of uniform pattern modes and that the relative phases and amplitudes of these modes can be adjusted to form a narrow beam. Then the beam is scanned by adjusting the currents feeding the Butler matrix. This is only qualitatively correct; the patterns calculated from the actual current distribution established on the array by the matrix differ from the patterns formed from the ideal modes. There is reasonable agreement between the calculated patterns and those obtained experimentally with a 32-element array of dipoles used to demonstrate how a beam could be formed and then scanned. The inputs to the Butler matrix required to achieve a prescribed cophasal sector distribution on the array are determined from the synthesis procedure of Davies with the corresponding changes in the current distribution on the array for other beam positions.

DD FORM 1 NOV 65 1473 (PAGE 1)

S/N 0101-807-6801

Security Classification

Security Classification

14. KEY WORDS	LINK A ROLE	LINK A WT	LINK B ROLE	LINK B WT	LINK C ROLE	LINK C WT
Radar systems						
Communication systems						
Antennas						
Radiation patterns						
Continuous scanning						
Circular arrays						
Beam-forming matrices						

DD FORM 1 NOV 65 1473 (BACK)
(PAGE 2)

Security Classification